PHYSICAL REVIEW C VOLUME 25, NUMBER 1 JANUARY 1982

Resonating-group study of the ^{3}He(^{3}H)+α systems: Bound states to 113 MeV

Robert D. Furber
Space Sensors Division, Hughes Aircraft Company, Culver City, California 90230

Ronald E. Brown
Los Alamos National Laboratory, Los Alamos, New Mexico 87545

G. L. Peterson,* D. R. Thompson,† and Y. C. Tang
School of Physics, University of Minnesota, Minneapolis, Minnesota 55455
(Received 27 July 1981)

An effective nucleon-nucleon spin-orbit force is included in a single-channel resonating-group calculation for the ^{3}He(^{3}H)+α system up to a c.m. energy of 113.1 MeV. The parameters of the spin-orbit force were chosen to reproduce the phase shifts for $p+\alpha$ scattering at low energies and the bound-state properties of ^{7}Li and ^{7}Be. A phenomenological, parity-dependent imaginary potential is used to account for reaction channels. The calculation gives a reasonable account of the experimental differential cross sections and analyzing powers available in this energy region.

[NUCLEAR REACTIONS ^{3}He(^{3}H)+α, bound states to 113.1 MeV (c.m.); calculated elastic differential cross sections and analyzing powers; resonating-group method.]

I. INTRODUCTION

The resonating-group method[1,2] (RGM) has been used successfully to describe reactions and scattering for a large variety of nuclear systems. In particular, such studies have elucidated the connection between the nucleon-nucleon force and the nucleus-nucleus interaction and have made major contributions toward understanding the role played by the Pauli exclusion principle. It has been pointed out[3] that investigations of the mass-7 system have been very fruitful in this respect, especially in view of the strong exchange effects that exist there.[4] Thus, a considerable amount of work has been done in reference to the RGM on this system,[5–15] the latest being a calculation[16] of the ^{3}He(α,γ)^{7}Be capture reaction at low energies, which is relevant to branching in the proton-proton reaction chain[17,18] in stars and the solar neutrino problem.[19]

In the present work we have augmented the formalism described in Ref. 14 by including a noncentral part to the nucleon-nucleon force used in our RGM calculation for the ^{3}He(^{3}H)+α system. We have also extended the calculation and its comparison with experiment up to a c.m. energy of 113.1 MeV. Part of this work has been described in a Ph.D. thesis.[20]

II. FORMULATION

Much of the present formulation follows that of Ref. 14. This includes (1) the mass-4 and mass-3 wave functions, (2) the central nucleon-nucleon potentials, both nuclear and Coulomb, and (3) the parity-dependent imaginary potential. The reader is referred to Ref. 14 for details. We only comment here that with respect to item (1) because the nucleon-nucleon force we use is nonsaturating, we fix the parameters in the wave functions to yield the correct rms matter radii for the α particle, the triton, and the ^{3}He nucleus; with respect to item (2) the central interaction yields the proper low-energy, nucleon-nucleon scattering parameters and gives the correct spin-orbit-averaged energies for the $^2P_{3/2}$ and $^2P_{1/2}$ bound states of ^{7}Be and ^{7}Li; and with respect to item (3) two parameters, the strength U_0 and parity dependence C_I, in the phenomenological imaginary potential are adjusted at each energy to aid in fitting the experimental elastic differential cross section. This corrects

crudely for the single-channel nature of the calculation.

In the present study we add a noncentral component to the nucleon-nucleon force; namely, the following spin-orbit potential $V_{ij}(\mathrm{so})$,

$$V_{ij}(\mathrm{so}) = -(V_0 + V_\tau \vec{\tau}_i \cdot \vec{\tau}_j)(\vec{\mathrm{r}}_i - \vec{\mathrm{r}}_j) \times (\vec{\mathrm{p}}_i - \vec{\mathrm{p}}_j)\cdot(\vec{\sigma}_i + \vec{\sigma}_j)(2\hbar)^{-1} \times \exp(-\lambda r_{ij}^2) , \quad (1)$$

where $r_{ij} = |\vec{\mathrm{r}}_i - \vec{\mathrm{r}}_j|$ is the distance between nucleon i and nucleon j. This potential contains two strength parameters V_0 and V_τ and one range parameter λ. Equation (1) is to be viewed as an effective noncentral potential and not as the true nucleon-nucleon spin-orbit potential. This is because the more complicated, but important, nucleon-nucleon tensor interaction is not taken into account, and it is desired that Eq. (1) compensate as much as possible for this omission.

In order to fix the parameters of Eq. (1), the $^2P_{3/2}$-$^2P_{1/2}$ bound-state splittings in ^{7}Be and ^{7}Li were calculated for a range of parameter values. In addition, an RGM calculation for $p+\alpha$ scattering was carried out along the lines indicated in Refs. 21 and 22, and the phase shifts below the reaction threshold were studied for a range of parameter values. Although there was no parameter set that gave best fits simultaneously to the mass-5 and mass-7 data, the following values yield a good compromise:

$$V_0 = -50 \text{ MeV}, \quad V_\tau = 270 \text{ MeV}, \quad \lambda = 2 \text{ fm}^{-2} . \quad (2)$$

TABLE I. Bound-state results for ^{7}Be and ^{7}Li using the noncentral potential of Eqs. (1) and (2) and the central potential of Ref. 14. The binding energies are in MeV and are referenced to the $\alpha+{}^3$H and $\alpha+{}^3$He breakup energies.

Nucleus	State	Binding energy Calculation	Experiment
^{7}Be	$^2P_{3/2}$	1.63	1.59
^{7}Be	$^2P_{1/2}$	1.07	1.16
^{7}Li	$^2P_{3/2}$	2.53	2.47
^{7}Li	$^2P_{1/2}$	1.93	1.99

The final results for the mass-7 bound states are given in Table I. The low-energy $p+\alpha$ phase shifts are not shown here, but the results are very similar to those given in the appropriate figures of Refs. 21 and 22. We do, however, show in Fig. 1 a calculation of the polarization transfer coefficient[23] $K_z^{x'}$ (which is identical to the Wolfenstein parameter A) as compared with the data of Ref. 24. This comparison has not been published before, and it is seen that the noncentral force of Eqs. (1) and (2) does quite well in reproducing the data of Ref. 24.

Finally, the form of the RGM, partial-wave-expanded, integrodifferential equation for the radial part $f_{Jl}(r)$ of the relative-motion function is given in Ref. 21. Here we include the imaginary potential iW of Ref. 14 to obtain

$$\left\{\frac{\hbar^2}{2\mu}\left[\frac{d^2}{dr^2} - \frac{l(l+1)}{r^2}\right] + E - V_N(r) - V_C(r) - i[1 + C_I(-1)^l]U(r) - \eta_{Jl} V_{\mathrm{so}}(r)\right\} f_{Jl}(r) = \int_0^\infty [k_l^N(r,r') + k_l^C(r,r') + \eta_{Jl} k_l^{\mathrm{so}}(r,r')] f_{Jl}(r')\, dr' , \quad (3)$$

with

$$\eta_{l+1/2,l} = l, \quad \eta_{l-1/2,l} = -(l+1) . \quad (4)$$

In Eq. (3) μ is the reduced mass; V_N and k_l^N are the direct potential and exchange kernel, respectively, arising from the nuclear part of the nucleon-nucleon central force (k_l^N also contains the kinetic-energy exchange terms); V_C and k_l^C are the direct potential and exchange kernel, respectively, arising from the Coulomb part of the nucleon-nucleon force; and V_{so} and k_l^{so} are the direct potential and exchange kernel, respectively, arising from the nucleon-nucleon noncentral force of Eq. (1). The radial function $U(r)$ occurring in the imaginary potential and the Coulomb kernel k_l^C are

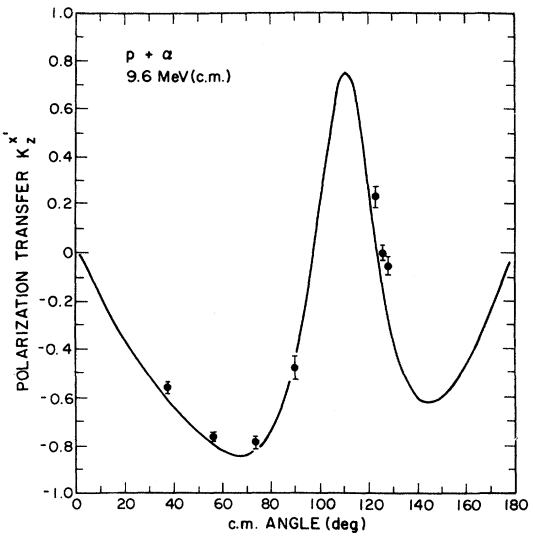

FIG. 1. Polarization transfer coefficient $K_z^{x'}$ for $p+\alpha$ scattering at 9.6 MeV (c.m.). This coefficient is identical to the Wolfenstein parameter A (Ref. 23). The curve is from an RGM calculation and the data (points) are from Ref. 24.

given in Ref. 14, and V_C has the form given in Ref. 5. Because the nucleon-nucleon central force used here[14] is not the same as that used in Ref. 5, the expressions for V_N and k_l^N are not identical to those given there. However, the modifications to the formulas of Ref. 5 are relatively simple and can be implemented in the manner indicated in the Appendix of Ref. 21. The spin-orbit terms V_{so} and k_l^{so} which we derived for the present work are given in the Appendix.

III. RESULTS AND DISCUSSION

A. S matrix

We write the S matrix for our problem in the form

$$S_l^{\pm} = |S_l^{\pm}| e^{2i\delta_l^{\pm}}, \tag{5}$$

where the superscript $+$ means $J=l+\frac{1}{2}$ and $-$ means $J=l-\frac{1}{2}$, and the phase shift $\delta_l^{\pm}$ is a real number. The relationships between $S_l^{\pm}$ and observable quantities are given, e.g., in Ref. 25.

In Fig. 2 we show the phase shift δ_l^+ vs c.m. energy for $^3He+\alpha$ scattering. The well known odd-even effect[7,26,27] produced by the Pauli exclusion principle is evident from the clustering in pairs of the l (even) with the $l+1$ (odd) phases, and it is seen that the effect for this nuclear system is such that the interaction in odd-l states is more attractive than in even-l states. In the inset is displayed the reasonably good agreement we obtain with the empirical phases of Ref. 28 for the $^2F_{7/2}$ and $^2F_{5/2}$ resonances. The phase-shift splittings are shown in Fig. 3, where it is seen that the splittings are generally rather small, except for resonance effects in the $l=3$ and 4 partial waves.

The amplitudes $|S_l^+|$ and the amplitude splittings are illustrated in Figs. 4 and 5. The amplitudes differ from unity because of the use of the phenomenological imaginary potential in the calculation. In Fig. 6 we show an Argand plot of S_l^+ at 60.2 MeV (c.m.). The counterclockwise rotation of the odd-l pattern with respect to the even-l pattern, resulting in a close proximity of odd-l to even-l points, is a manifestation of the odd-even effect mentioned above.

Figure 7 compares the RGM phases δ_l^+ at 17.09 MeV (c.m.) with the empirical phases of solution C from Ref. 29, which solution used RGM phases[20] as starting values in the search process. Again the odd-even effect appears, this time as a characteristic zigzag pattern in both the calculated and empirical phases. The other two solutions (A and B) of Ref. 29 show very little odd-even effect and also yield somewhat higher overall values of χ^2 than the value for solution C. From a theoretical point of view, the "true" solution should exhibit a marked odd-even effect, and therefore we would suggest that solution C is the most physically realistic of the three.

B. Level analysis

Because of the cluster structure of the wave function used, the present calculation should reveal mass-7 levels having a large partial width for α decay. From Fig. 2 we note significant resonance structure in the $l=2-5$ partial waves. We use the R-matrix formalism[30] to extract somewhat more quantitative information than is given by plots of the phase shifts versus energy. We consider $l=2$, 4, and 5; the $l=3$ resonances have been thoroughly considered in Ref. 28. We perform a two-level, single-channel analysis, where the first level is associated with the resonance and the second level is a background level to aid in representing the nonresonant part of the phase shift. We follow the same procedure that was used in Ref. 31 for the

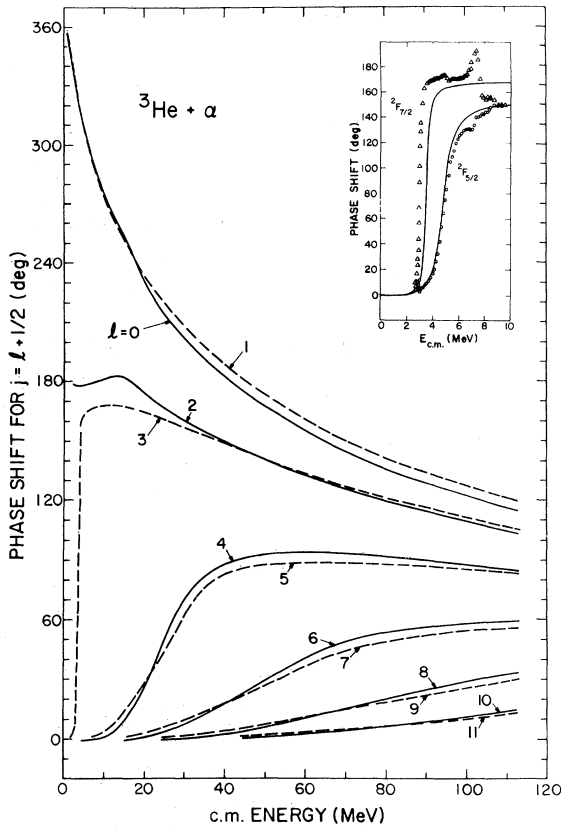

FIG. 2. Phase shifts δ_l^+ for ^{3}He+α scattering from the present calculation. The inset shows a comparison of calculated (curves) and empirical (points, Ref. 28) phases near the $l=3$ resonances.

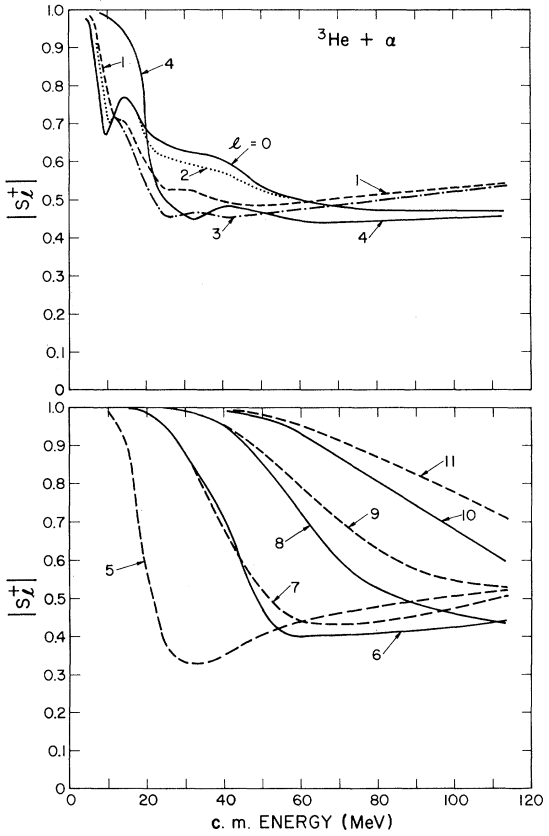

FIG. 4. Amplitudes of the ^{3}He+α S matrix for $J=l+\frac{1}{2}$ from the present calculation.

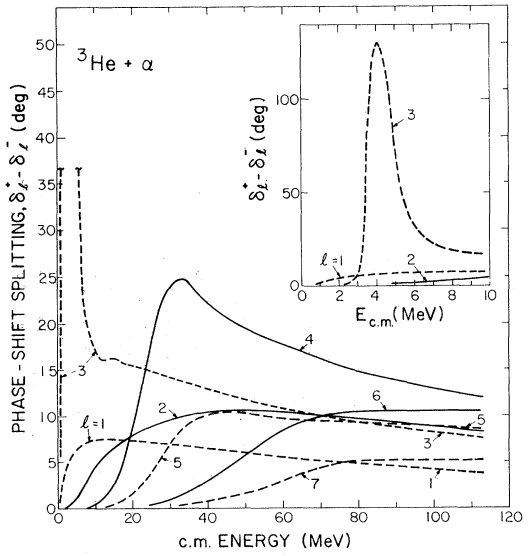

FIG. 3. J splitting of the ^{3}He+α phase shifts from the present calculation. The inset shows the region of the $l=3$ resonances.

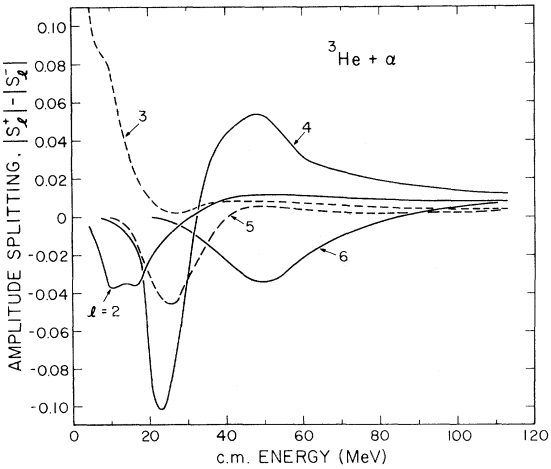

FIG. 5. J splitting of the ^{3}He+α S-matrix amplitudes from the present calculation. Any partial waves not shown have splittings that fall between $+0.02$ and -0.02 over the entire energy range.

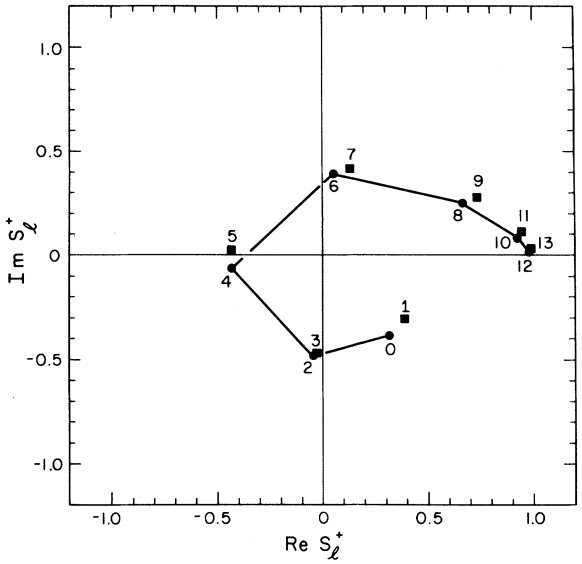

FIG. 6. Argand plot of the S matrix for $J=l+\frac{1}{2}$ at 60.2 MeV (c.m.). The quantum numbers l are indicated, and the even-l values are connected by straight lines.

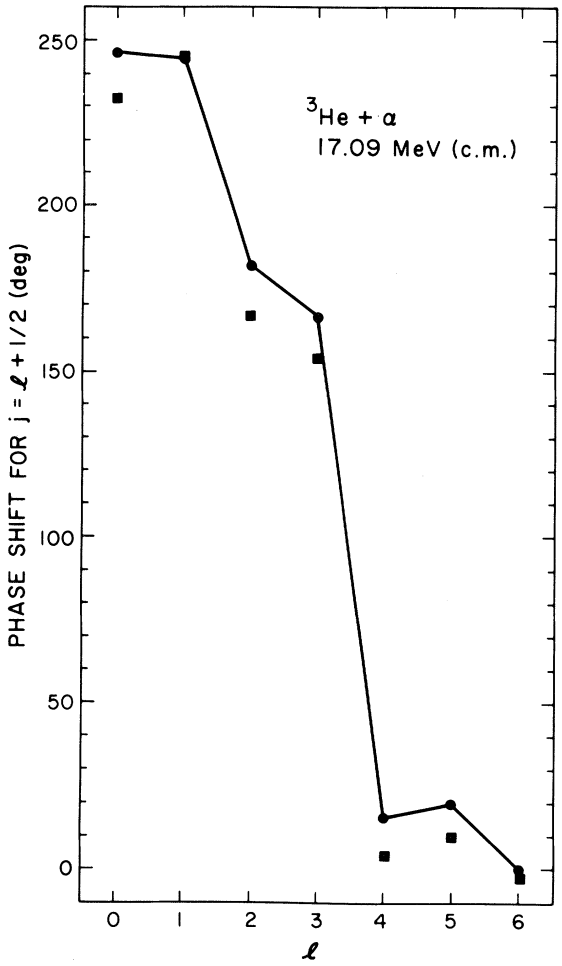

FIG. 7. Phase shifts δ_l^+ for ^{3}He+α scattering at 17.09 MeV (c.m.). The points connected by straight lines are from the present calculation, and the other points are from the empirical phase-shift solution C of Ref. 29.

$\alpha+\alpha$ system. Thus, a fit is carried out for several values of the channel radius a, and a value for a is chosen that is in the broad minimum which exists in the functional relationship of χ^2 to a. The boundary condition parameter B is chosen so that the level shift at the resonance energy E_r is zero. The results of the analysis are given in Table II. The values of E_r and Γ for ^{7}Be are reasonable when compared with Fig. 2.

C. Differential cross sections and analyzing powers

The results for the bound states have already been discussed and are presented in Table I. As in Ref. 14, the parameters U_0 and C_I of the imaginary potential in Eq. (3) were adjusted until a good visual fit to the elastic differential cross section was obtained. In particular, the calculated curve was required, where feasible, to agree with the cross sections in the regions of relative maxima. An illustration of the effect of varying U_0 and C_I independently is given in Fig. 2 of Ref. 14. The parameters used, along with the resulting total reaction cross sections,[32] are listed in Table III. Other values that are not given in Table III, but which were used in constructing Figs. 2–7, were taken from Refs. 14 and 20. As has been noted many times in the past, the inclusion of the imaginary potential in a light system does not significantly affect the calculated phase shifts $\delta_l^\pm$ of Eq. (5), nor does it appreciably change the angular shape of the differential cross section; its main effect is to lower the magnitude of the calculated cross section. Partial waves up to $l_{\max}=11$ were used in the calculations up to 44.5 MeV (c.m.), $l_{\max}=13$ was used at 44.5 MeV (c.m.), and $l_{\max}=19$ was used for the higher energies.

In Figs. 8 and 9 we compare calculations with experimental (Refs. 8, 9, 12, 28, and 33) ^{3}He+α

TABLE II. R-matrix parameters from a two-level analysis of RGM phases for the mass-7 system. a is the channel radius, B is the boundary condition parameter, E_r is the resonance energy, γ_r^2 is the α-particle reduced width for the resonance, Γ is the total width of the resonance, E_λ is the level energy for the background level, and γ_λ^2 is its α-particle reduced width.

Nucleus	Level	a (fm)	B	E_r (MeV)	γ_r^2 (MeV)	Γ (MeV)	E_λ (MeV)	γ_λ^2 (MeV)
^{7}Be	$^2D_{5/2}$	5.0	−0.253	8.8	1.4	9	33	2.5
	$^2D_{3/2}$	5.0	−0.241	9.2	1.5	10	35	2.6
	$^2G_{9/2}$	4.0	−0.654	22	2.2	14	62	5.2
	$^2G_{7/2}$	4.0	−0.584	24	2.4	17	69	5.5
	$^2H_{11/2}$	4.5	−0.857	23	2.7	18	147	23
	$^2H_{9/2}$	4.5	−0.824	24	2.8	19	242	40
^{7}Li	$^2D_{5/2}$	5.0	−0.238	8.1	1.4	9	32	2.5
	$^2D_{3/2}$	5.0	−0.227	8.4	1.5	10	34	2.6
	$^2G_{9/2}$	4.0	−0.649	21	2.1	13	60	5.0
	$^2G_{7/2}$	4.0	−0.578	23	2.4	17	68	5.4
	$^2H_{11/2}$	4.5	−0.852	23	2.7	18	125	19
	$^2H_{9/2}$	4.5	−0.819	23	2.8	19	187	30

elastic differential cross sections over a broad energy range. Generally, the calculation does quite well in reproducing the experimental cross sections. The strong exchange nature of the ^{3}He+α interaction is illustrated by the large rise in the cross section at backward angles. At the higher energies there is an increasingly clear separation into forward-angle direct scattering and backward-angle exchange scattering, both in the data and in the calculation. We should stress that in the calculation the exchange processes arise very naturally through the use of a fully antisymmetrized wave function. One rather curious discrepancy occurs at 60.2 MeV (c.m.), where the calculated minimum is not very close in angle to the experimental minimum in the cross section. This is unusual in RGM calculations, in which we usually find that the angle at which the minimum occurs is well reproduced by the calculation, even though the magnitude of the cross section at the minimum might not be.

TABLE III. Values of the parameters of the imaginary potential. C_I is the strength of the parity dependence [Eq. (3)] and U_0 is the strength of $U(r)$ [Eq. (3)], which has the volume-plus-derivative, Woods-Saxon form defined in Ref. 14. Also given are the total reaction cross sections σ_R produced by these parameters. Values not listed here that were used to construct Figs. 2–7 were taken from Refs. 14 and 20.

c.m. energy (MeV)	U_0 (MeV)	C_I	σ_R (mb)
4.98	0.05	0	90
10.14	0.95	−0.3	301
24.36	2.50	−0.6	465
44.5	3.70	−0.35	456
60.2	4.50	−0.2	461
80.0	5.00	−0.1	445
113.1	5.50	0	418

In Fig. 10 we compare calculated cross sections and analyzing powers with experimental data[9,29,34]; $t+\alpha$ at 9.69 MeV (c.m.) and ^{3}He+α at 17.09 MeV (c.m.). The calculated analyzing powers are not unreasonable. The forward-angle discrepancy for ^{3}He+α tends to lessen at somewhat higher energies, because the calculation then develops a more distinct minimum near 40°. The calculated $t+\alpha$ analyzing power seems less satisfactory; however, it is known[35] that with rather small changes from the RGM phases, an excellent fit can be generated. A comparison of RGM ^{3}He+α cross sections and analyzing powers with experiment in the c.m. energy range 10–18 MeV is presented in Ref. 29.

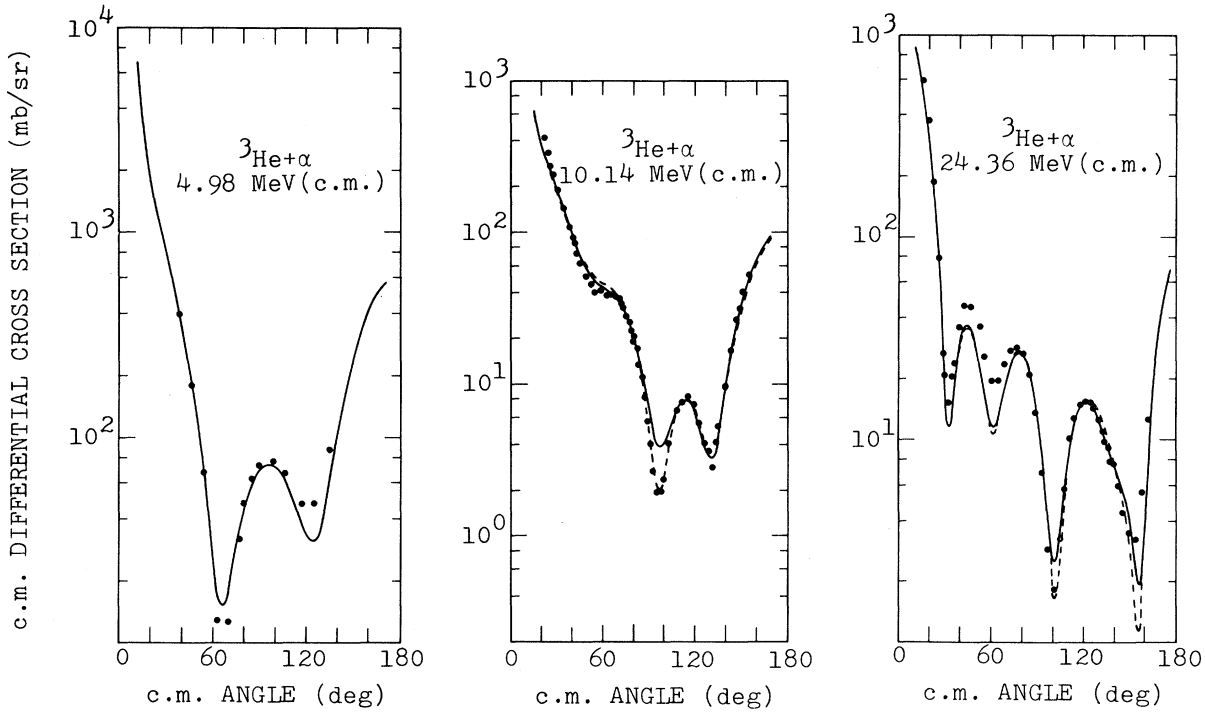

FIG. 8. Differential cross sections for ^{3}He+α elastic scattering. The solid curves are from the present calculation and the dashed curves show the effect of omitting the exchange-Coulomb term k_f^C. The data (points) are from Ref. 28 (4.98 MeV), Ref. 9 (10.14 MeV), and Ref. 8 (24.36 MeV).

Finally, in Fig. 11 we show a prediction of the ^{3}He+α analyzing power at 60.2 MeV (c.m.). The occurrence of a large negative analyzing power near 90° (c.m.), which is in the region of interference between direct and exchange scattering, seems to be a fairly general feature (see, e.g., Fig. 10 and Ref. 29).

IV. CONCLUSION

The mass-7 system has undergone extensive study with the RGM over the past years (Refs. 1–16, 20, 29, and 32). In the present RGM calculation we have included a noncentral nucleon-nucleon interaction, namely, an effective spin-orbit potential. The low-energy properties of the mass-5 and mass-7 systems were used to fix the parameters of that potential, and this resulted in a very successful description of the mass-7 system all the way up to 113.1 MeV (c.m.). Analyzing-power measurements for $t+\alpha$ or ^{3}He+α above 20 MeV (c.m.) would be very useful in further testing these calculations (e.g., see the prediction in Fig. 11). Of course, there are improvements that could be made in the calculation, the major one being the inclusion of a nucleon-nucleon tensor interaction, together with the appropriate modifications of the cluster internal wave functions. If that were done, then the parameters of both the tensor and spin-orbit interactions could be adjusted to values consistent with nucleon-nucleon data, and the resulting RGM calculation would be less empirically based than is the present one.

This work was supported by the U.S. Department of Energy.

APPENDIX: EXPRESSIONS FOR THE SPIN-ORBIT INTERACTIONS $V_{so}(r)$ AND $k_f^{so}(r,r')$ OF EQUATION (3)

The expression for the direct spin-orbit potential is

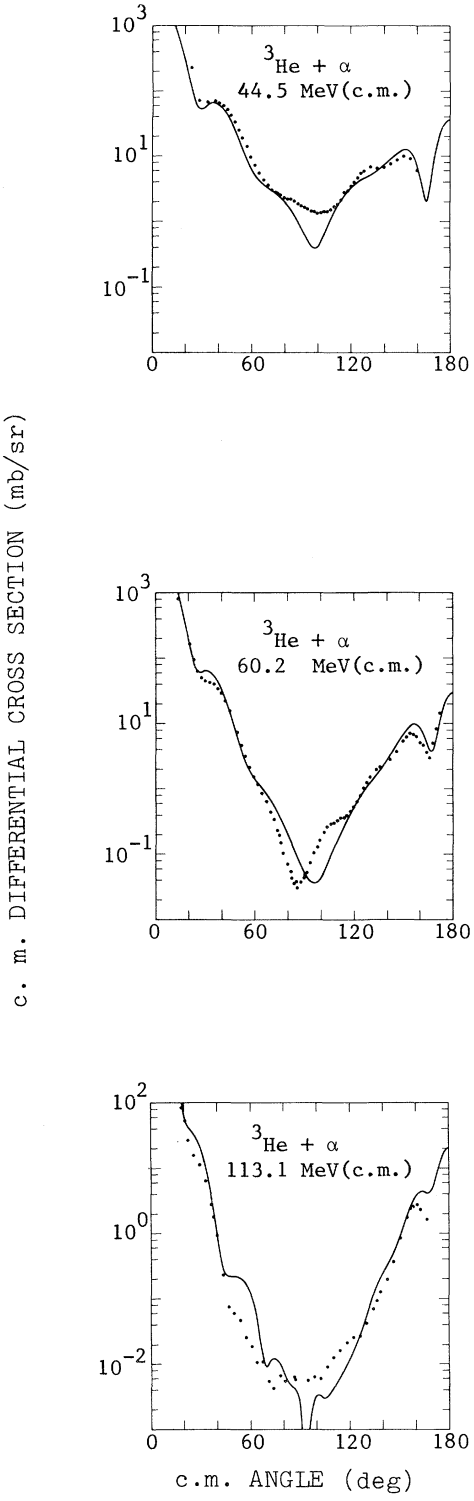

FIG. 9. Differential cross sections for ^{3}He+α elastic scattering. The curves are from the present calculation, and the data are from Ref. 12 (44.5 MeV) and Ref. 33 (60.2 and 113.1 MeV).

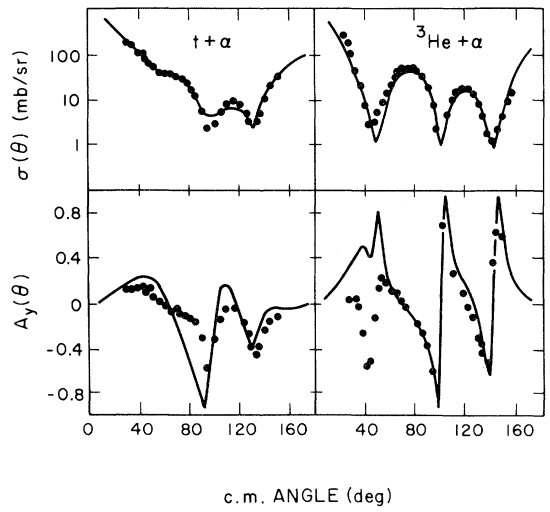

FIG. 10. c.m. differential cross sections $\sigma(\theta)$ and analyzing powers $A_y(\theta)$ for $t+\alpha$ scattering at 9.69 MeV (c.m.) and for ^{3}He+α scattering at 17.09 MeV (c.m.). The curves are from the present calculation, and the experimental data are indicated by points. The $t+\alpha$ data are from Ref. 34, the ^{3}He+α cross section is from Ref. 9, and the ^{3}He+α analyzing power is from Ref. 29.

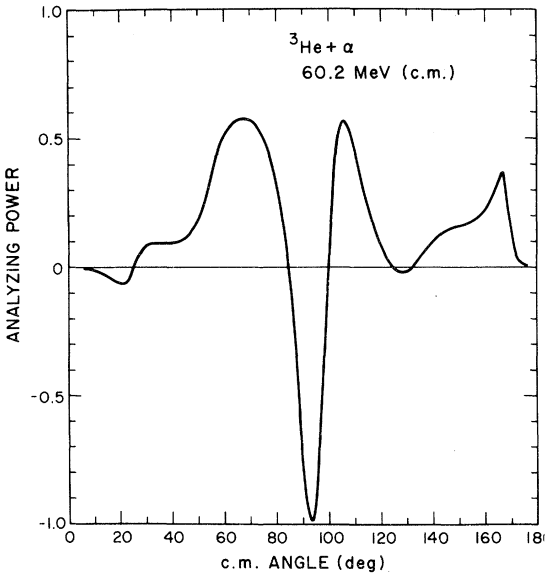

FIG. 11. Prediction from the present calculation of the analyzing power for ^{3}He+α scattering at 60.2 MeV (c.m.).

$$V_{so}(r)=-\tfrac{7}{6}V_0\left[\frac{12\alpha\bar{\alpha}}{12\alpha\bar{\alpha}+\lambda[8\alpha+9\bar{\alpha}]}\right]^{5/2}\exp\left[-\frac{12\alpha\bar{\alpha}\lambda}{12\alpha\bar{\alpha}+\lambda[8\alpha+9\bar{\alpha}]}r^2\right], \tag{A1}$$

where α and $\bar{\alpha}$ are the size parameters of the mass-4 and mass-3 nuclei, respectively. In Ref. 14 these size parameters are defined, and their values are determined so that the wave functions yield the correct rms matter radii for the α particle, the triton, and the ^{3}He nucleus.

In order to list the exchange kernel $k_l^{so}(r,r')$ it is convenient to define a variety of quantities. First, we define the following constants in terms of α, $\bar{\alpha}$, and λ:

$$\beta_{mn}=m\alpha+n\bar{\alpha}; \tag{A2}$$

$$t_{15}^1=\beta_{89},\quad e_{15}^1=\frac{72\alpha^2+96\alpha\bar{\alpha}+72\bar{\alpha}^2}{7t_{15}^1}+\frac{48}{7}\lambda,$$

$$s_{15}^1=-\frac{48\alpha\bar{\alpha}}{t_{15}^1e_{15}^1},\quad g_{15}^1=\left[\frac{12\alpha\bar{\alpha}}{\pi t_{15}^1}\right]^{3/2},$$

$$d_{15}^1=\frac{36\alpha^2+97\alpha\bar{\alpha}+36\bar{\alpha}^2}{7t_{15}^1}+\frac{24}{7}\lambda; \tag{A3}$$

$$t_{26}^1=\alpha\bar{\alpha}\beta_{89}+2\lambda\beta_{11}\beta_{23},$$

$$e_{26}^1=\frac{\alpha\bar{\alpha}(72\alpha^2+96\alpha\bar{\alpha}+72\bar{\alpha}^2)+2\lambda\beta_{11}(18\alpha^2-6\alpha\bar{\alpha}+24\bar{\alpha}^2)}{7t_{26}^1},$$

$$s_{26}^1=\frac{12\alpha\bar{\alpha}\beta_{11}{}^2}{t_{26}^1e_{26}^1},\quad g_{26}^1=\left[\frac{12\alpha^2\bar{\alpha}^2}{\pi t_{26}^1}\right]^{3/2},$$

$$d_{26}^1=\frac{\alpha\bar{\alpha}(36\alpha^2+97\alpha\bar{\alpha}+36\bar{\alpha}^2)+2\lambda\beta_{11}(9\alpha^2+46\alpha\bar{\alpha}+12\bar{\alpha}^2)}{7t_{26}^1}; \tag{A4}$$

$$t_{15}^2=\beta_{23}(\beta_{11}+2\lambda),$$

$$e_{15}^2=\frac{\beta_{11}(6\alpha^2-36\alpha\bar{\alpha}+6\bar{\alpha}^2)+\lambda(36\alpha^2-12\alpha\bar{\alpha}+48\bar{\alpha}^2)}{7t_{15}^2},$$

$$s_{15}^2=-\frac{12\alpha\bar{\alpha}\beta_{11}}{t_{15}^2e_{15}^2},\quad g_{15}^2=\left[\frac{12\alpha^2\bar{\alpha}^2}{\pi\beta_{11}t_{15}^2}\right]^{3/2},$$

$$d_{15}^2=\frac{\beta_{11}(3\alpha^2+31\alpha\bar{\alpha}+3\bar{\alpha}^2)+\lambda(18\alpha^2+92\alpha\bar{\alpha}+24\bar{\alpha}^2)}{7t_{15}^2}; \tag{A5}$$

$$t_{37}^2=4\alpha\beta_{23}+6\lambda\beta_{11},$$

$$e_{37}^2=\frac{4\alpha(6\alpha^2-36\alpha\bar{\alpha}+6\bar{\alpha}^2)+\lambda(-276\alpha^2-264\alpha\bar{\alpha}+12\bar{\alpha}^2)}{7t_{37}^2},$$

$$s_{37}^2=\frac{12\alpha\beta_{11}{}^2}{t_{37}^2e_{37}^2},\quad g_{37}^2=\left[\frac{48\alpha^3\bar{\alpha}^2}{\pi\beta_{11}{}^2t_{37}^2}\right]^{3/2},$$

$$d_{37}^2=\frac{4\alpha(3\alpha^2+31\alpha\bar{\alpha}+3\bar{\alpha}^2)+\lambda(156\alpha^2+162\alpha\bar{\alpha}+6\bar{\alpha}^2)}{7t_{37}^2}; \tag{A6}$$

$$t_{15}^3=3\beta_{11}+8\lambda,$$

$$e_{15}^3=-\frac{144\alpha\beta_{11}+\lambda(368\alpha-16\bar{\alpha})}{7t_{15}^3},$$

$$s_{15}^3=-\frac{16\alpha\beta_{11}}{t_{15}^3e_{15}^3},\quad g_{15}^3=\left[\frac{64\alpha^3\bar{\alpha}^2}{\pi\beta_{11}{}^3t_{15}^3}\right]^{3/2},$$

$$d_{15}^3=\frac{75\alpha\beta_{11}+\lambda(208\alpha+8\bar{\alpha})}{7t_{15}^3}. \tag{A7}$$

We will also make use of the function $S_l(x)$, which depends on r and r' and is defined by

$$S_l(x)=\frac{4\pi}{x}\mathcal{J}_{l+1/2}(xrr') , \tag{A8}$$

where $\mathcal{J}_\nu(z)$ is a hyperbolic, spherical Bessel function. It satisfies the recursion relation

$$\mathcal{J}_{\nu+1}(z)=\mathcal{J}_{\nu-1}(z)+\frac{2\nu}{z}\mathcal{J}_\nu(z) , \tag{A9}$$

with

$$\mathcal{J}_{1/2}(z)=\sinh z,\quad \mathcal{J}_{3/2}(z)=\frac{\sinh z}{z}-\cosh z , \tag{A10}$$

and is related to the Bessel function of the first kind J_ν by

$$\mathcal{J}_\nu(z)=i^{\nu-1}\sqrt{(\tfrac{1}{2}\pi z)}\,J_\nu(iz) . \tag{A11}$$

Employing the constants defined in Eqs. (A3)–(A7) and the functions S_l of Eq. (A8), we display the spin-orbit kernel as follows:

$$\begin{aligned}k_l^{so}(r,r')=(\tfrac{12}{7})^3\{&(V_0+3V_\tau)s_{15}^1 g_{15}^1 S_l(-\tfrac{6}{7}e_{15}^1)\exp[-\tfrac{6}{7}d_{15}^1(r^2+r'^2)]\\&+2(V_0+3V_\tau)s_{26}^1 g_{26}^1 S_l(-\tfrac{6}{7}e_{26}^1)\exp[-\tfrac{6}{7}d_{26}^1(r^2+r'^2)]\\&-4V_0 s_{15}^2 g_{15}^2 S_l(-\tfrac{6}{7}e_{15}^2)\exp[-\tfrac{6}{7}d_{15}^2(r^2+r'^2)]\\&-6V_\tau s_{37}^2 g_{37}^2 S_l(-\tfrac{6}{7}e_{37}^2)\exp[-\tfrac{6}{7}d_{37}^2(r^2+r'^2)]\\&+3(V_0-V_\tau)s_{15}^3 g_{15}^3 S_l(-\tfrac{6}{7}e_{15}^3)\exp[-\tfrac{6}{7}d_{15}^3(r^2+r'^2)]\}\ .\end{aligned} \tag{A12}$$

---

*Present address: Physics Department, University of Texas, Dallas, Texas 75200.

†Present address: Applied Physics Laboratory, Johns Hopkins University, Laurel, Maryland 20810.

[1]K. Wildermuth and Y. C. Tang, *A Unified Theory of the Nucleus* (Vieweg, Braunschweig, Germany, 1977).

[2]Y. C. Tang, M. LeMere, and D. R. Thompson, Phys. Rep. 47, 167 (1978).

[3]R. E. Brown, in *Clustering Aspects of Nuclear Structure and Nuclear Reactions (Winnipeg, 1978),* Proceedings of the Third International Conference on Clustering Aspects of Nuclear Structure and Nuclear Reactions, edited by W. T. H. van Oers, J. P. Svenne, J. S. C. McKee, and W. R. Falk (AIP, New York, 1978), p. 90.

[4]Y. C. Tang and R. E. Brown, Phys. Rev. C 4, 1979 (1971).

[5]Y. C. Tang, E. Schmid, and K. Wildermuth, Phys. Rev. 131, 2631 (1963).

[6]E. J. Wurster-Kanellopoulos, University of Tübingen Technical Report No. BMwF-FB K67-69, 1967 (unpublished).

[7]R. E. Brown and Y. C. Tang, Phys. Rev. 176, 1235 (1968).

[8]P. Schwandt, B. W. Ridley, S. Hayakawa, L. Put, and J. J. Kraushaar, Phys. Lett. 30B, 30 (1969).

[9]C. G. Jacobs, Jr., and R. E. Brown, Phys. Rev. C 1, 1615 (1970).

[10]R. E. Brown, E. E. Gross, and A. van der Woude, Phys. Rev. Lett. 25, 1346 (1970); 25, 1668 (1970).

[11]W. Fetscher, K. Sattler, N. C. Schmeing, E. Seibt, Ch. Weddigen, and E. J. Kanellopoulos, Phys. Lett. 34B, 171 (1971).

[12]W. Fetscher, E. Seibt, Ch. Weddigen, and E. J. Kanellopoulos, Phys. Lett. 35B, 31 (1971).

[13]W. Fetscher, E. Seibt, and Ch. Weddigen, Nucl. Phys. A216, 47 (1973).

[14]J. A. Koepke, R. E. Brown, Y. C. Tang, and D. R. Thompson, Phys. Rev. C 9, 823 (1974).

[15]J. A. Koepke and R. E. Brown, Phys. Rev. C 16, 18 (1977).

[16]Q. K. K. Liu, H. Kanada, and Y. C. Tang, Phys. Rev. C 23, 645 (1981).

[17]R. W. Kavanaugh, in *Cosmology, Fusion & Other Matters* (George Gamow Memorial Volume), edited by F. Reines (Colorado Associated University Press, 1972), p. 169.

[18]C. Rolfs and H. P. Trautvetter, Annu. Rev. Nucl. Part. Sci. 28, 115 (1978).

[19]J. N. Bahcall, S. H. Lubow, W. F. Huebner, N. H. Magee, Jr., A. L. Merts, M. F. Argo, P. D. Parker, B. Rozsnyai, and R. K. Ulrich, Phys. Rev. Lett. 45, 945

(1980).
[20]R. D. Furber, Ph.D. thesis, University of Minnesota, 1976 (unpublished).
[21]I. Reichstein and Y. C. Tang, Nucl. Phys. A158, 529 (1970).
[22]D. R. Thompson, I. Reichstein, W. McClure, and Y. C. Tang, Phys. Rev. 185, 1351 (1969).
[23]G. G. Ohlsen, Rep. Prog. Phys. 35, 717 (1972).
[24]P. W. Keaton, Jr., D. D. Armstrong, R. A. Hardekopf, P. M. Kurjan, and Y. K. Lee, Phys. Rev. Lett. 29, 880 (1972).
[25]D. R. Thompson, Y. C. Tang, and R. E. Brown, Phys. Rev. C 5, 1939 (1972).
[26]R. E. Brown, F. S. Chwieroth, Y. C. Tang, and D. R. Thompson, Nucl. Phys. A230, 189 (1974).
[27]M. LeMere and Y. C. Tang, see Ref. 3, p. 538.
[28]R. J. Spiger and T. A. Tombrello, Phys. Rev. 163, 964 (1967); R. J. Spiger, Ph.D. thesis, California Institute of Technology, 1967 (unpublished).
[29]Y. -W. Lui, O. Karban, A. K. Basak, C. O. Blyth, J. M. Nelson, and S. Roman, Nucl. Phys. A297, 189 (1978).
[30]A. M. Lane and R. G. Thomas, Rev. Mod. Phys. 30, 257 (1958).
[31]W. S. Chien and R. E. Brown, Phys. Rev. C 10, 1767 (1974).
[32]For a discussion of total reaction cross sections with respect to calculations with a central force only, see J. A. Koepke and R. E. Brown, Phys. Rev. C 16, 18 (1977).
[33]P. G. Roos, A. Nadasen, P. E. Frisbee, N. S. Chant, T. A. Carey, M. T. Collins, and B. Th. Leeman, Phys. Rev. C 21, 799 (1980). The Argand plot in Fig. 3 of this reference is for an optical potential having a stronger attraction in the even than in the odd partial waves. However, it is reported that equally good fits to the experimental cross sections were obtained with either sign for the exchange potential, and therefore an Argand plot could just as well have been presented for a potential for which the odd partial waves show the stronger attraction. In that case Fig. 3 would have appeared very similar to our Fig. 6.
[34]N. Jarmie, F. D. Correll, R. E. Brown, R. A. Hardekopf, and G. G. Ohlsen, Los Alamos Scientific Laboratory Report No. LA-8492, 1980.
[35]N. Jarmie and F. D. Correll, private communication.